Cell Host & Microbe, Volume *16*

Supplemental Information

Proline Isomerization of the Immune Receptor-Interacting Protein RIN4 by a Cyclophilin Inhibits Effector-Triggered Immunity in *Arabidopsis*

Meng Li, Xiqing Ma, Yi-Hsuan Chiang, Koste A. Yadeta, Pengfei Ding, Liansai Dong, Yan Zhao, Xiuming Li, Yufei Yu, Ling Zhang, Qian-Hua Shen, Bin Xia, Gitta Coaker, Dong Liu, and Jian-Min Zhou

SUPPLEMENTAL INFORMATION

Binary Constructs,

35S::*ROC1-FLAG*, 35S::*RIN4*, 35S::*RPM1-HA*, and 35S::*RPS2-HA* were generated by PCR-amplifying coding regions of *ROC1*, *RIN4*, *RPM1*, and *RPS2*, and inserted into pCAMBIA 1300 under the control of the 35S promoter. To generate the WT *RIN4* construct containing the native promoter, the *RIN4* genomic DNA was PCR-amplified from Col-0 plants and introduced into the pCAMBIA 1300. Site-directed mutagenesis was used to introduce various mutations into the *ROC1* and *RIN4* constructs. The coding regions of *RIN4, ROC1, RPM1,* and *RPS2* were PCR-amplified and inserted into pCAMBIA1300 vectors containing Cluc and Nluc (Chen et al., 2009) to generate *Cluc-RIN4, RPM1-Nluc, RPM1-Cluc, RPS2-Nluc, RPS2-Cluc, ROC1-Nluc, and ROC1-Cluc* constructs. *AvrB-FLAG*, *AvrAC-HA*, and *mAvrAC-HA*, which carries a H469A substitution, were also inserted into pCAMBIA1300. The 35S::*ROC1-GFP* and 35S::*BFP-RIN4* constructs were generated by PCR-amplifying coding regions of *ROC1, RIN4,* enhanced *GFP,* and *BFP*, and inserted into the pCAMBIA1300-221 vector. Above constructs were introduced into *Agrobacterium* GV3101. 35S::*T7-RIN4*, 35S::*T7-RIN4*^{T166D}, and 35S::*T7-RIN4*^{P149VT166D} were cloned into pENTR/D-TOPO vector (Invitrogen) and moved into the gateway compatible p1776 destination vector, and introduced into *Agrobacterium* strain C58C1.

Recombinant Proteins,

His-tagged AvrRpt2 and RIN4 were constructed by inserting coding sequences into the pET28A plasmid (Novagen). GST-ROC1 was constructed by inserting the ROC1 coding sequence into the pGEX-6P-1 plasmid (GE Healthcare Life Science). Mutations were introduced into RIN4 and ROC1 by site directed mutagenesis. The resulting constructs were

introduced into *Escherichia coli*, and His- and GST-tagged recombinant proteins were purified by Ni+-sepharose (Qiagen) and glutathione agarose affinity chromatography, respectively.

SUPPLEMENTAL FIGURES

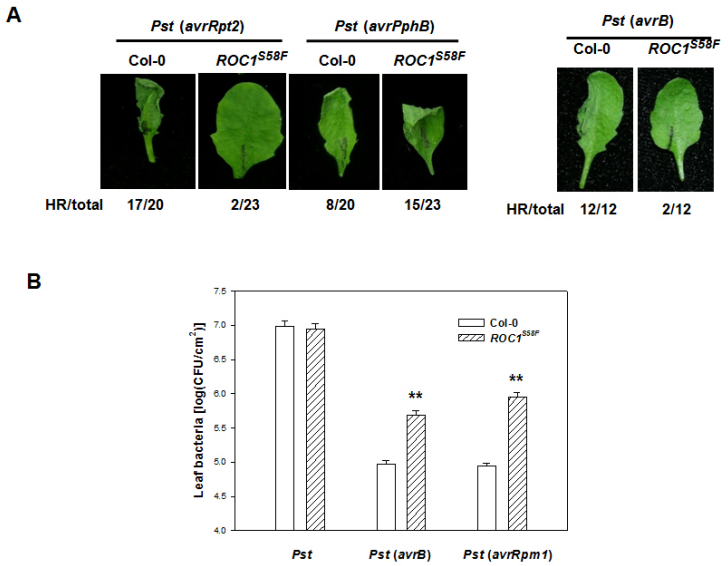

Figure S1. The *ROC1*^{S58F} Mutant Is Compromised in RPS2- and RPM1-Specified Resistance in Arabidopsis (related to Figure 1). (**A**). The *ROC1*^{S58F} mutant is compromised in HR triggered by *Pst* (*avrRpt2*) and *Pst* (*avrB*), but displays normal HR in response to *Pst* (*avrPphB*). Leaves of WT (Col-0) and *ROC1*^{S58F} plants were infiltrated with 5×10^7 CFU/ml *Pst* (*avrRpt2*), *Pst* (*avrPphB*), and *Pst* (*avrB*), and HR was photographed at 8, 8, and 4 h later, respectively. The numbers below the photograph indicate ratio of number of leaves showing HR to total number of infiltrated leaves. (**B**). The *ROC1*^{S58F} mutant is compromised in resistance to *Pst* (*avrRpm1*). Leaves of WT (Col-0) and *ROC1*^{S58F} plants were infiltrated with 10^6 CFU/ml *Pst, Pst* (*avrB*), and *Pst* (*avrRpm1*) bacteria, and leaf bacterial population was measured 3 days post-inoculation. Error bars represent standard deviation (n=8, 2 biological repeats).

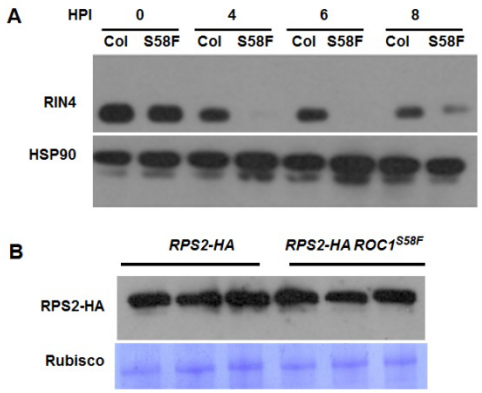

Figure S2. The *ROC1*^{S58F} Mutant Shows Enhanced RIN4 Cleavage by AvrRpt2 and Normal RPS2 Accumulation (related to Figure 2). (**A**). The *ROC1*^{S58F} mutant display enhanced RIN4 cleavage upon *Pst* (*avrRpt2*) inoculation. WT and *ROC1*^{S58F} mutant plants were infiltrated with DC3000 (*avrRpt2*) at 2×10^7 CFU/ml for the indicated times, and amounts of RIN4 protein in the total protein extract was determined by immune blot with anti-RIN4 antibodies. The amounts of HSP90 protein detected by immune blot show equal loading of proteins in lanes. (**B**). RPS2-HA protein level in transgenic *RPS2-HA* plants and *ROC1*^{S58F} *RPS2-HA* plants. CBB stain of Rubisco indicates equal loading of protein in lanes.

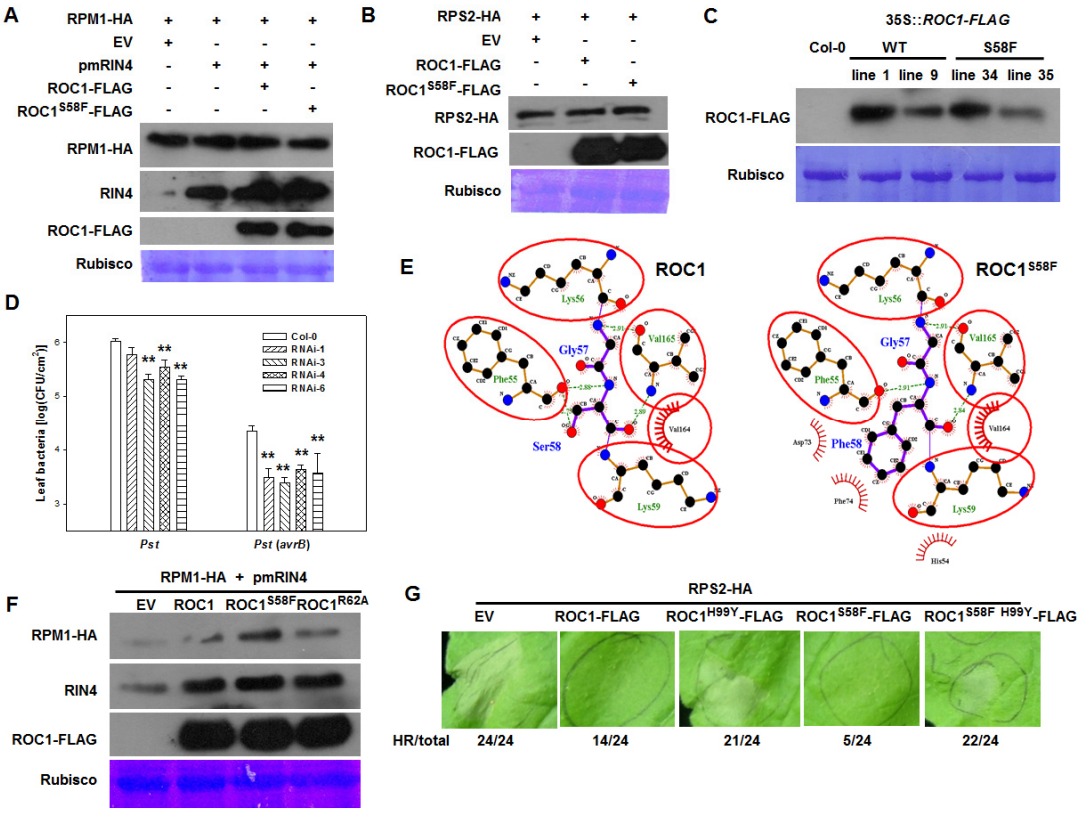

Figure S3. ROC1 Inhibits RPM1- and RPS2-Specified HR (related to Figure 3). (**A** and **B**). Accumulation of RPM1-HA, RPS2-HA, RIN4, and ROC1-FLAG proteins in *Nb* leaves shown in Figures 3A and 3B. (**C**). Accumulation of ROC1-FLAG protein in stable transgenic Arabidopsis plants shown in Figure 3C. CBB stain of Rubisco indicate equal loading of protein in lanes. (**D**). *ROC1* RNAi lines display increased resistance to *Pst* (*avrB*) bacteria. Bacteria were infiltrated into the indicated plants, and bacterial population in the leaf was determined 3 days post inoculation. Plants used in this experiment were grown under long day condition (16 h light/8 h darkness). Error bars represent standard deviation (n=8, 2 biological repeats). (**E**). The ROC1^{S58F} mutation results in new interactions between Phe58 and Lys59 with surrounding amino acids. The structures of WT ROC1 and ROC1^{S58F} were modeled by using SWISS-MODEL (Arnold et al., 2006), and the interactions surrounding aa58 are

presented as LIGPLOT (Laskowski et al., 2011) diagram. Thatched semi-circles indicate van der Waals contacts. Hydrogen bonds are shown as green dashed lines. Note that the S58F substitution results in a loss of a hydrogen bond between the oxygen atom of Ser58 and the oxygen atom in Phe55 and brings in new interactions between Phe58 and Asp73 and Phe74, and between Lys59 and His54 through van der Waals contacts. (**F**). Accumulation of RPM1-HA, RIN4, and ROC1-FLAG proteins in *Nb* leaves shown in Figures 3E. (**G**). ROC1 His99 is required for the inhibition of RPS2 HR in *Nb* plants. *Nb* leaves were infiltrated with *Agrobacterium* carrying the indicated constructs, and HR was photographed 48 h after infiltration. Numbers below the photograph indicate ratio of HR to total number of infiltration.

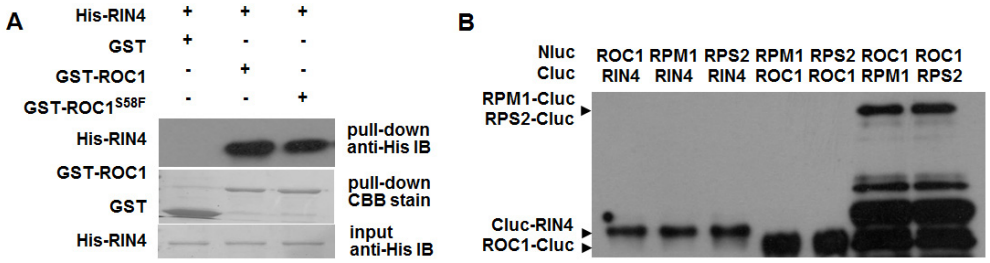

Figure S4. ROC1 Interacts with RIN4 (related to Figure 4). (**A**). GST pull-down assay showing that ROC1 and ROC1^{S58F} interact equally with RIN4. (**B**). Accumulation of proteins in *Nb* plants transiently expressing the indicated constructs as shown in Figure 4B.

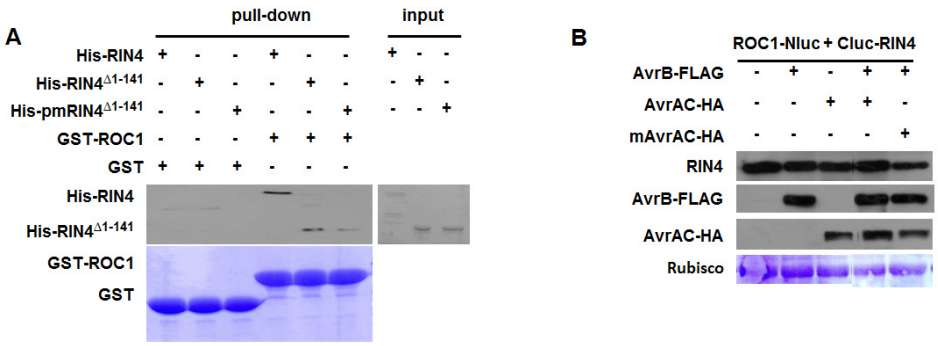

Figure S5. ROC1-RIN4 interaction is diminished upon RIN4 Thr166 phosphorylation (related to Fig. 5). (**A**). GST pull-down assay showing that the C terminus of RIN4 is sufficient for interaction with ROC1 and that the phospho-mimetic mutation reduces the interaction. (**B**). ROC1-RIN4 interaction in *N. benthamiana* plants is diminished by AvrB and restored by AvrAC. Shown are protein levels in *Nb* plants transiently expressing the indicated constructs, as shown in Figure 5B.

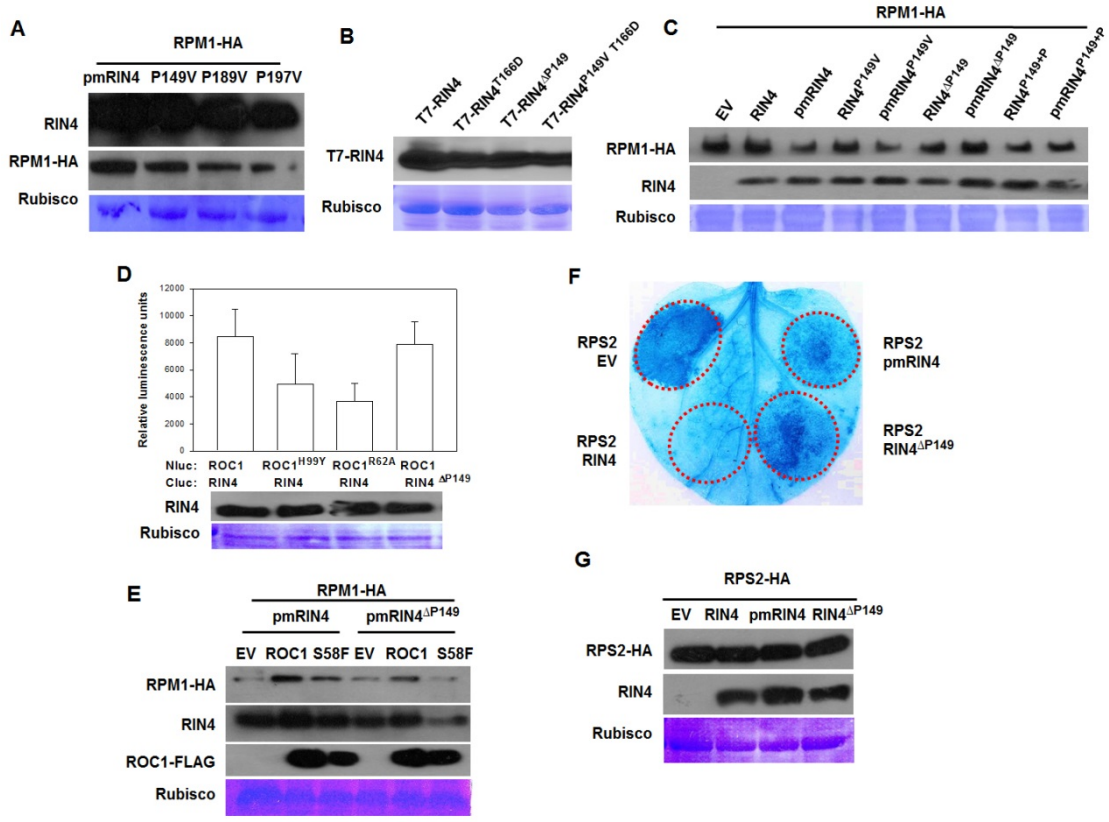

Figure S6. RIN4 Pro149 Plays A Critical Role in RPM1- and RPS2-Specified HR in *Nb* Plants (related to Figure 6). (**A-C**). Protein accumulation in *Nb* plants transiently expressing the indicated constructs, as shown in Figures 6A-6C. CBB stain of Rubisco indicated equal protein loading. (**D**). ROC1-RIN4 interaction is not affected by $RIN4^{\Delta P149}$. Error bars represent standard deviation (n=8, 2 biological repeats). (**E**). Protein accumulation in *Nb* plants transiently expressing the indicated constructs, as shown in Figure 6E. (**F**). pmRIN4 and $RIN4^{\Delta P149}$ are less capable of inhibiting RPS2-induced cell death in *N. benthamiana*. (**G**). Protein accumulation in *Nb* plants transiently expressing the indicated constructs, as shown in **F.**

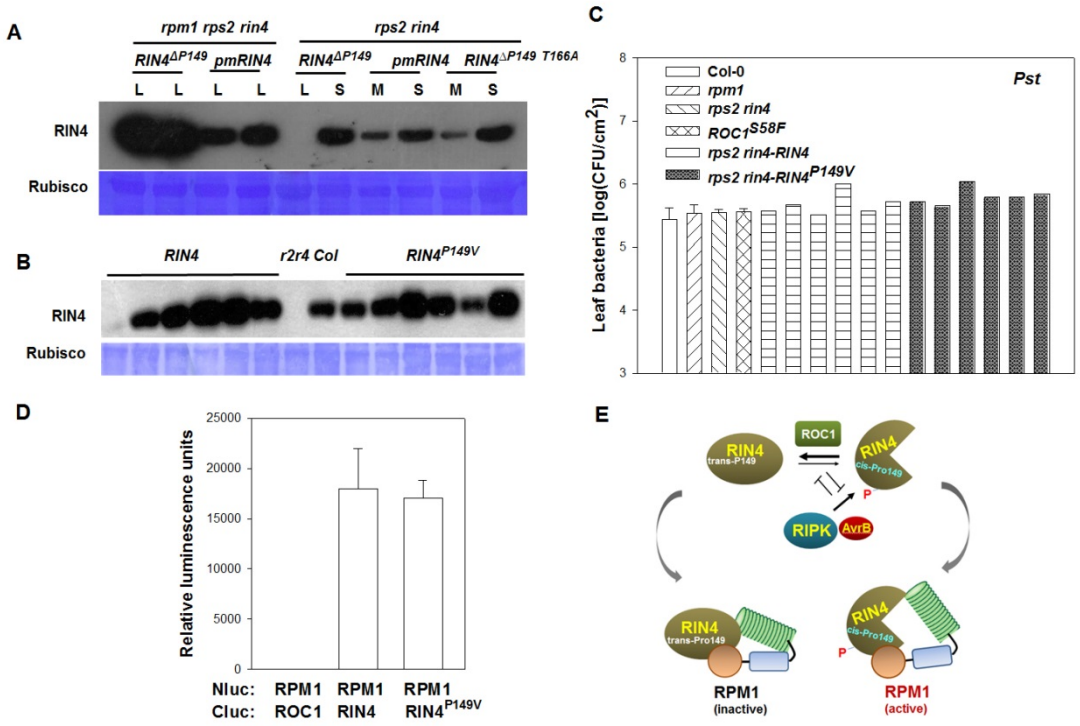

Figure S7. RIN4 Pro149 Controls RPM1 Activation in Arabidopsis (related to Figure 6).

(A-B**)**. Accumulation of the indicated RIN4 mutant proteins in T1 transgenic plants shown in Figure 7A-7B. In (**A**), selected T1 plants displaying large (L), medium (M), and small (S) sizes were examined for RIN4 accumulation by immuno blot. In (**B**), the WT *RIN4* and *RIN4*^{P149V} transgenes under the control of the native *RIN4* promoter were introduced into *rps2 rin4* (*r2r4*) double mutant, and the accumulation of the RIN4 protein in individual T1 transgenic plants was determined by immune blot. Col: Col-0 plants. CBB stain of Rubisco indicates amounts of total protein loaded in lanes. (**C**). *RIN4*^{P149V} transgenic plants are not affected in susceptibility to the virulent *Pst* bacteria. Individual T1 transgenic plants or non-transgenic plants of the indicated genotypes were inoculated with *Pst*, and bacterial population was determined 3 days post inoculation. Error bars indicate standard deviation (n=8, 2 biological repeats). (**D**). RIN4 and RIN4^{P149V} interact similarly with RPM1 in

luciferase complementation assay. Error bars represent standard deviation (n=8, 2 biological repeats). (**E**). Model for RPM1 regulation by ROC1 and RIN4. In the pre-activation state, ROC1 catalyzes RIN4 Pro149 isomerization. An interaction between RIN4 trans-isoform with RPM1 likely drives the reaction toward the *trans*-isoform, leading to the formation of an inactive RIN4-RPM1 complex. In the activation state, AvrB and RIPK induce the phosphorylation of RIN4 Thr166, rendering RIN4 a poor substrate of ROC1 because of a reduced RIN4-ROC1 interaction. This allows the accumulation of a pool of RIN4 *cis*-isoform, which forms an active RIN4-RPM1 complex and triggers resistance. Thus, the $RIN4^{P149V}$ mutant mimics the inactive, trans-isoform, whereas the $RIN4^{\Delta P149}$ mutant mimics the active, *cis*-isoform of RIN4. Please note that the Pro149 *cis*-isoform may enhance Thr166 phosphorylation (Figure 6F), whereas the *trans*-isoform may inhibit the phosphorylation (Figure 5C). The mutual inhibition of isomerization and phosphorylation may enforce the inactivation state prior to infection and activation state following infection.